24th COBEM - 2017

24th ABCM International Congress of Mechanical Engineering
December 3-8, 2017, Curitiba, PR, Brazil

COBEM-2017-2778
THE DEVELOPMENT OF A RACE CAR MONOCOQUE

Gustavo Gonçalves
Laura Farinasso Perucci
Rafael Peron de Marchi
USP - Universidade of São Paulo, EESC –School of Engineering of São Carlos, Av. Trab. São-Carlense, 400 - Parque Arnold Schimidt, São Carlos - SP, 13566-590, SP, Brasil
goncalves.engmec@gmail.com, lperucci53@gmail.com, rafael.marchi@usp.br

Abstract.*This paper aims to present the analysis and development of a chassis for an academic competition of Formula SAE (Society of Automotive Engineering). To achieve better handling and balance of the vehicle in relation to its predecessor project it was used the finite element analysis (FEA) for numerical simulation. Then the model was validated using experimental tests. During the design stage of the project several rule parameters were considered. Such as, safety for the pilot, torsional stiffness, chassis behavior in situations of cornering, accelerations and braking, free and forced vibrations as well as their respective free body and rigid body vibration modes. The present work also contemplates the steps of confection of the monocoque and the choice of the materials considering cost-benefit rate.*

Keywords:*Formula SAE, Chassi, Monocoque, FEA, E14*

1. INTRODUCTION

The biggest challenge in creating and building a chassis for a racing car lies in achieving a satisfactory relationship between strength, weight, stiffness and cost. To be able to correlate these parameters simultaneously becomes an arduous and complex task, because all the other subsystems of the vehicle depend exclusively on the final design of the chassis. All this work can be facilitated by the use of computing tools. One of them is finite element analisys (FEA) the aim of this work. The software used for all the simulations was the Ansys® Workbench v17. With this numerical method, it is possible to simplify the creation and optimization of Monocoque prototyping. Excluding the need to create several experimental models, since this requires time and money. Another important point is that the chassis model can not be reused, so every year is necessary to create a new model (Formula SAE Rules, 2017-18)

2. METODOLOGIA

We can divide the methodology of this work into two main parts, the first one being the numerical methodology where the techniques used to create the computational model of the monocoque are, and that we will refer to as E14 and the experimental methodology that was used to validate the computational model.

2.1 Numeric

In this part of the work we will present the simulations that correspond to the maneuvers executed by the car E14 being that of acceleration, braking, curve, braking with curve and braking with acceleration, also an analysis of torsional stiffness of the chassis and a modal analysis to validate the numerical model.

2.1.1 Creation of the computational model.

The geometry of the structure is defined by pilot positioning, safety rules established by the competition rules (Formula SAE Rules, 2017-18), Suspension, steering, engine and transmission hardpoints.

For the creation of the Computer Aided Design (CAD) model, a technique known as cloud of points was used that was connected by line segments as shown in Fig. (1). When using cloud of points to create the model, it is possible to guarantee that there will be no error of geometry, commonly generated by importing into commercial software.

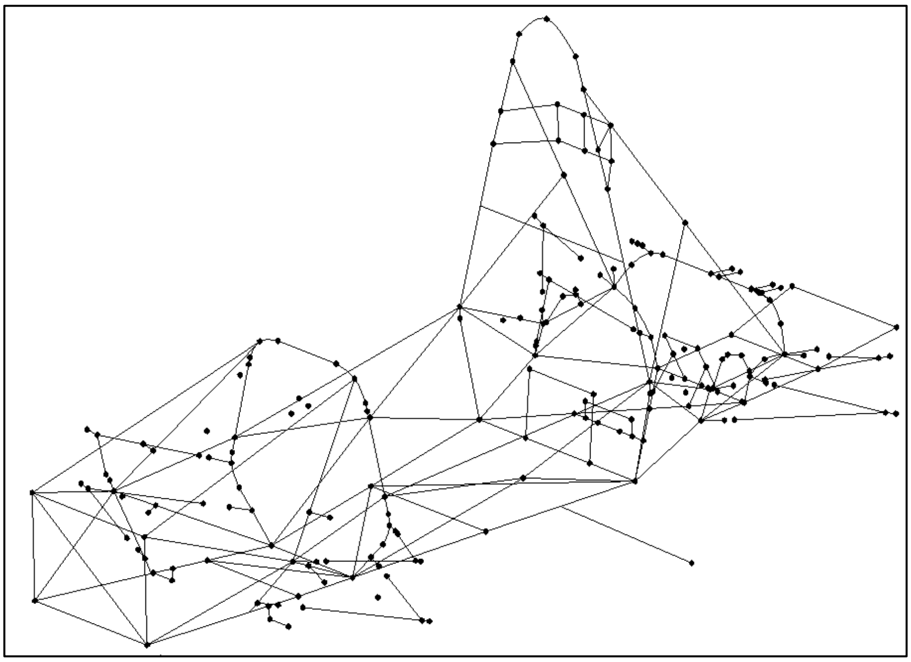

Figure 1: Isometric view of the chassis, cloud of interconnected points

These sequences are a way of representing the steel tubes of the chassis structure, so we defined the profiles of each of the tubes applied to the model that can be observed in Fig. (2). It is worth mentioning that in the design of the chassis E14 tubes with different diameter and thickness were used. Seeking to use the smallest thickness allowed by the rule (Formula SAE Rules, 2017-18).

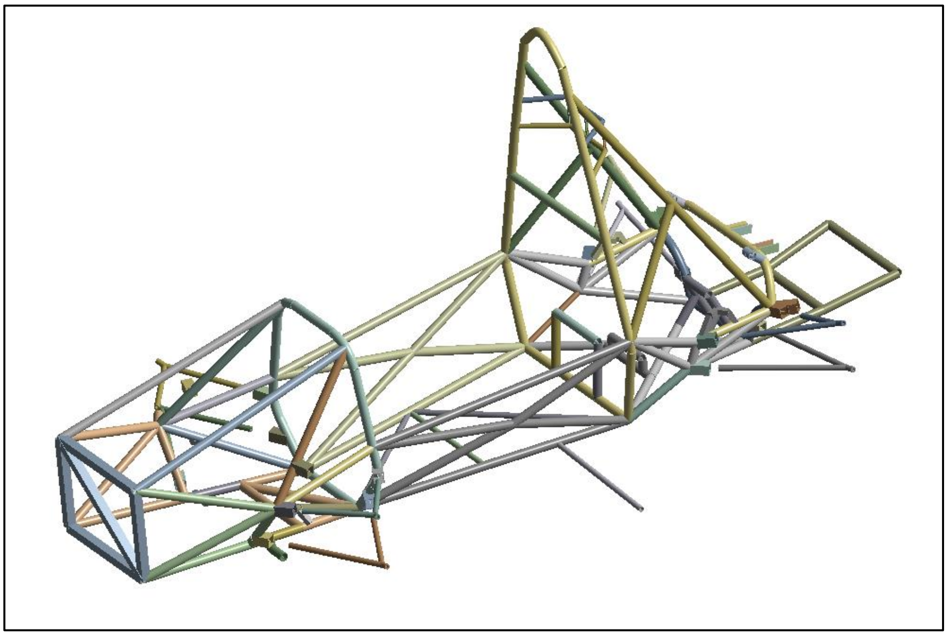

Figure 2: Tubes applied to the structure

Subsequently, the concentrated masses of the most relevant components of the car were added, as shown in Fig. (3), in order to make the simulation closer to the real model. The advantage of representing all components in the form of concentrated masses, instead of inserting the CAD model of the components themselves, makes the model simpler and numerically lighter.

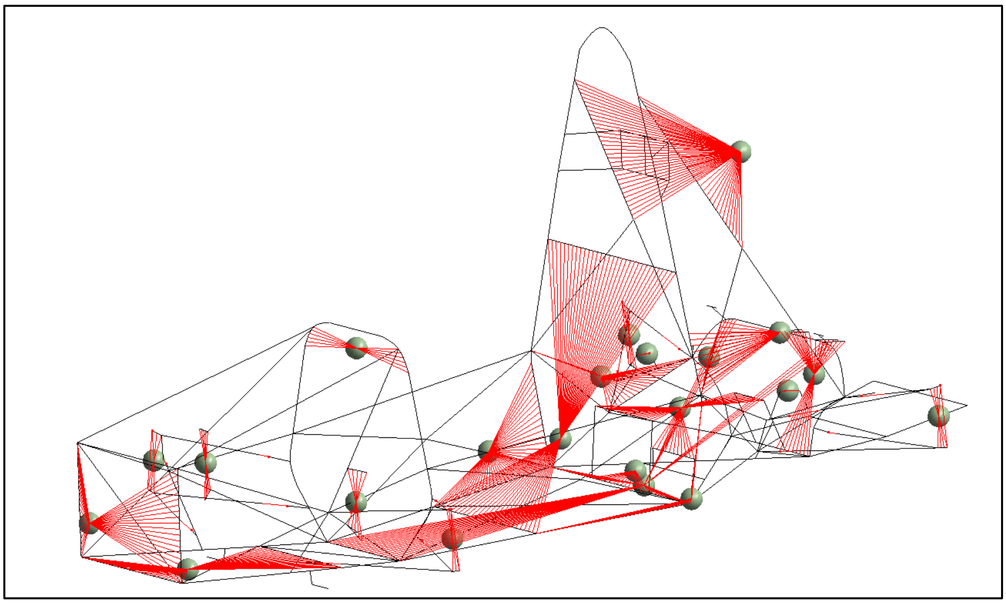

Figure 3: Masses set in the chassis representing the components and other systems of the vehicle.

After assigning the profiles of the tubes, the mesh elements that are presented in Fig. (4) were created, due to the great density of elements used to create the mesh, a small part of the chassis was enlarged for easier visualization.

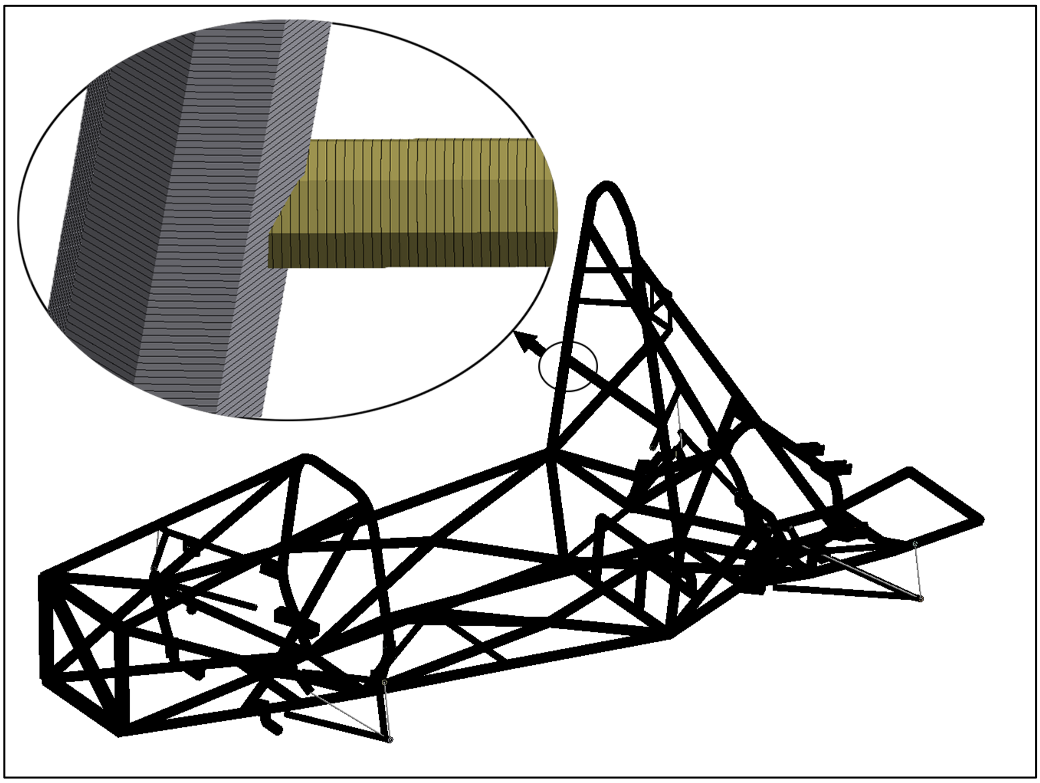

Figure 4: Mesh applied to the CAD model.

2.1.2 Contour Conditions.

The input parameters used to represent the critical conditions of the maneuvers were acquired from the data acquisition system of the prototype prior to E14. The values were taken from a diagram showing the accelerations of the car during a high performance test, as shown in Fig. (5). In addition, as recommended (D. Seward, 2014), the values obtained by a safety coefficient (1.3) because it is experimental data. The final values are shown in Tab. (1).

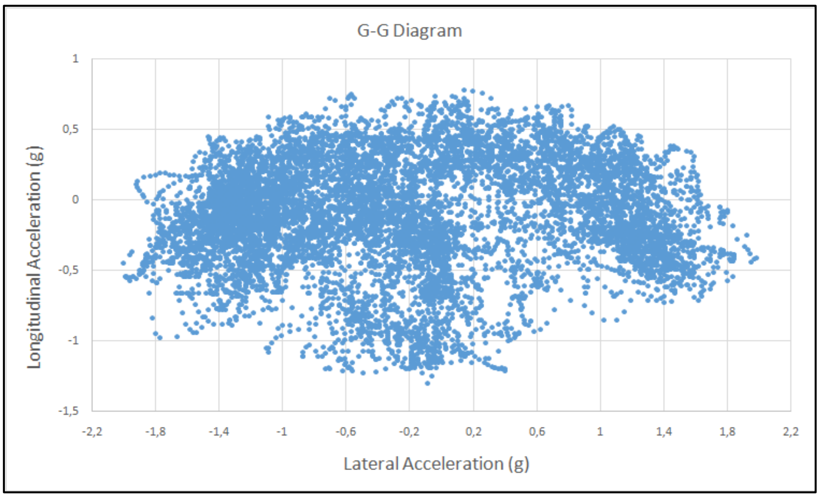

Figure 5. Diagram of car accelerations collected by the data acquisition system.

Table 1. Maximum on track acceleration values.

	Maximum Value	Corrected Value
Lateral Acceleration	2	2,6
Longitudinal Acceleration	0.78	1.014
Longitudinal Deceleration	-1.3	-1.69

For each type of simulation a different contour condition was created. As shown below:

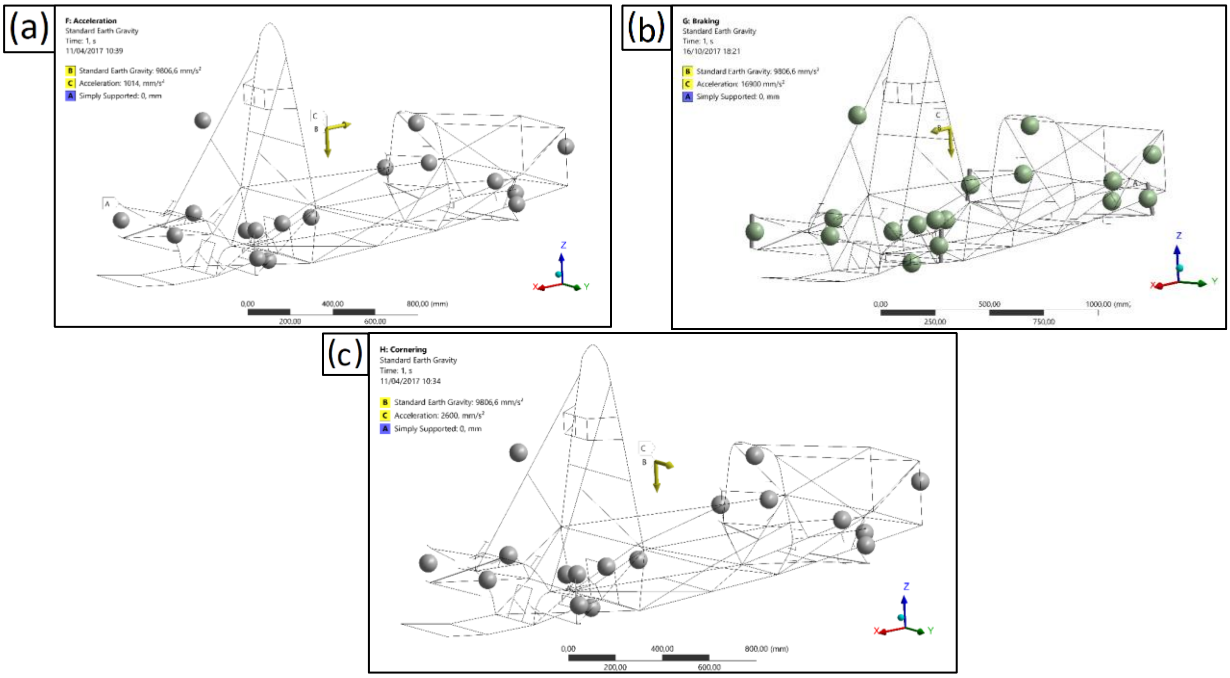

Figure 6: (a) Acceleration boundary condition applied to E14; (b) Braking Contour Condition Applied to E14; (c) Pure curve boundary condition applied to E14.

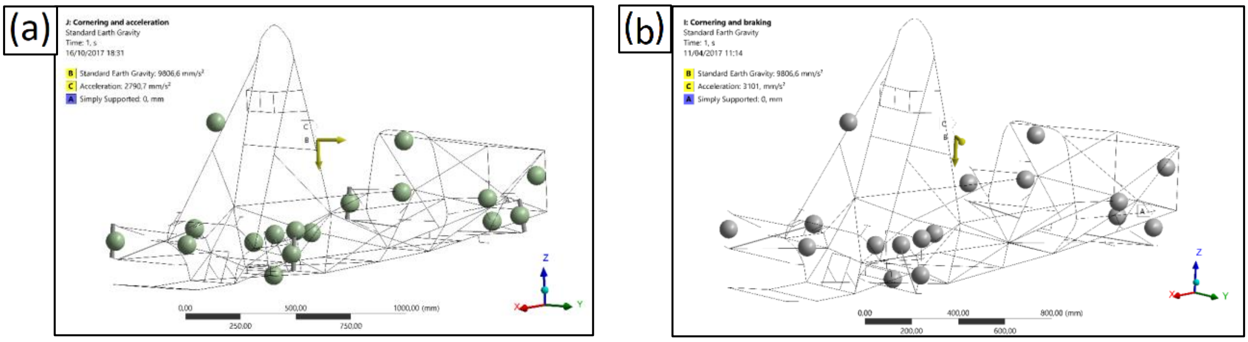

Figure 7: (a) Curve contour condition with acceleration applied to E14; (b) Curve Contour Condition with Braking.

Another condition in which we submitted the E14 model was in relation to the torsional stiffness. A binary force was applied to the front uprights and the rear uprights were fixed supported.

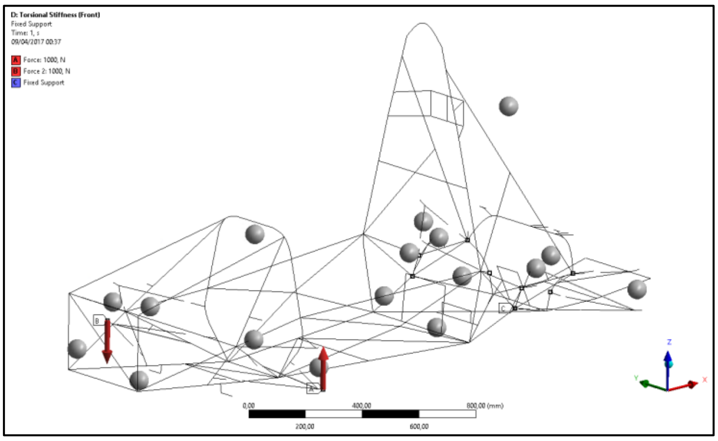

Figure 8: Frontal Torsional Stiffness boundary condition applied to E14

For the modal analysis, we used a free body type of simulation.

2.2 Experimental

For the torsional test in the E14 chassis, two supports were used to crimp, one for each rear uprights, a beam to connect the front uprights and apply force. The chassis torsion was obtained by measuring the difference of the angle of the Main Hoop and Rear Hoop compared to the starting position. The details of the test can be seen in Fig. (9). The rigidity was calculated from Eq. (1).

$$K = \frac{FL}{\tan^{-1}\left[\frac{(\Delta_{y1}+\Delta_{y2})}{2L}\right]} \tag{1}$$

If *K* is the torsional stiffness in *Nm / º*, *F* is the force applied, *L* is the gauge e $\frac{(\Delta_{y1}+\Delta_{y2})}{2}$ is the displacement of the structure (William, *et al*, 2001).

Figure 9. Torsional stiffness test.

To make modal assay, the structure was suspended by elastics to approach free body conditions and subsequently excited by magnetic shakers. The acquisition of frequencies was done using three accelerometers at each point of the structure, one for each coordinate axis (x, y, z).

.

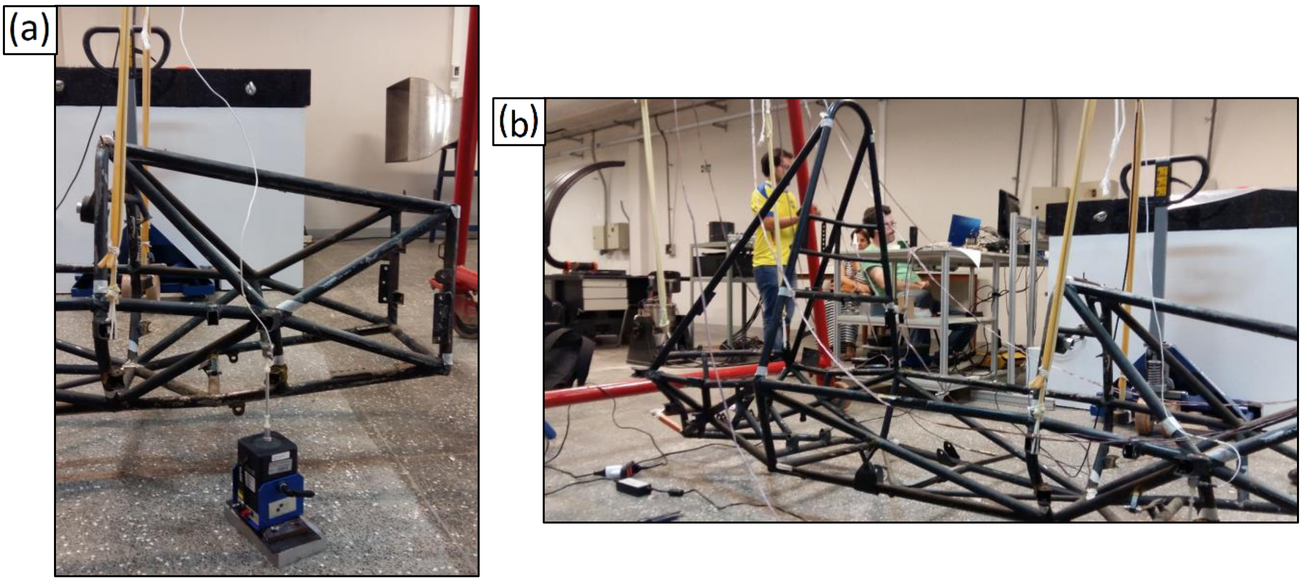

Figure 10. Modal test (a) magnetic shaker, (b) structure assembly.

3. RESULTS

To facilitate comprehension, the numerical and experimental results were separated.

3.1 Resultados Numéricos

From the structural simulations, we obtained the following results shown in Tab. (2).

Table 2. Maximum combined stress

	Maximum Combined Stress (MPa)
Acceleration	256.91
Braking	137.06
Cornering	121.45
Cornering and Acceleration	158.74
Cornering and Braking	110.05

The most critical case we obtained was pure acceleration. With maximum stress of 256.91MPa, the critical point can be seen in Fig. (11)(a). Fig. (11)(b) shows the point of maximum braking tension while Fig. (11) (c), pure curve.

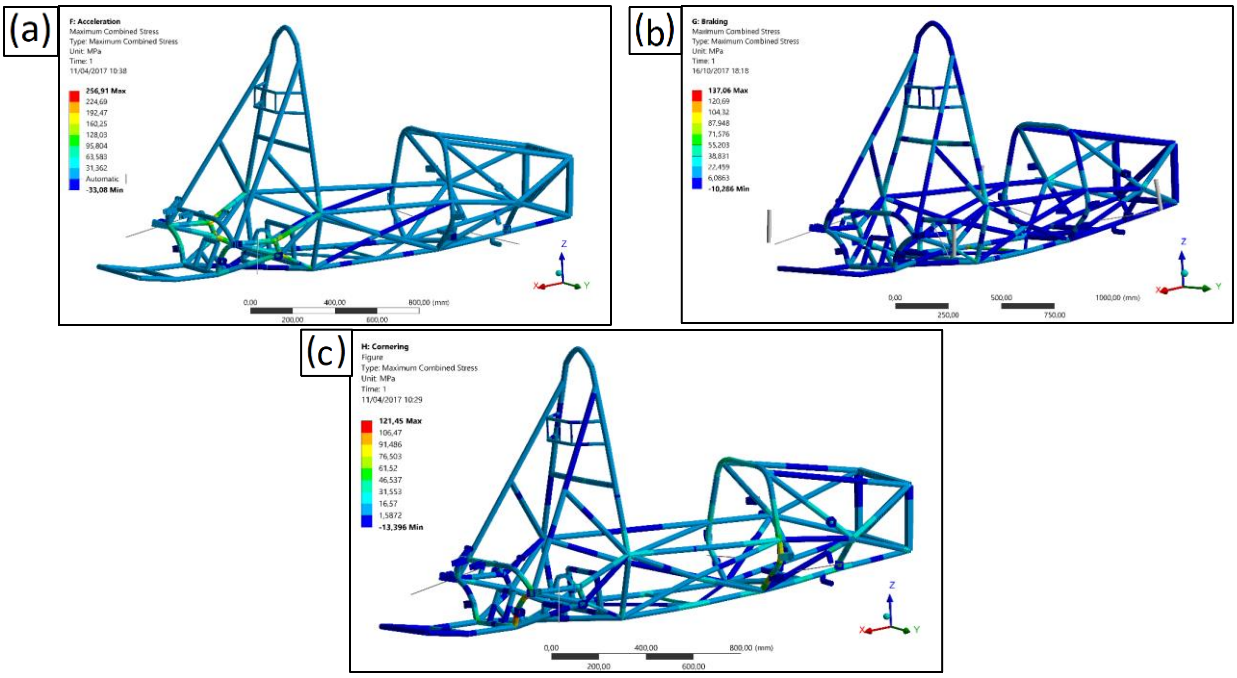

Figure 11. Maximum Combined Stress; (a) Acceleration, (b) Braking, (c) Cornering.

The combination of two maximum accelerations did not result in a higher tension, as can be seen in Fig. (12)(a),(b).

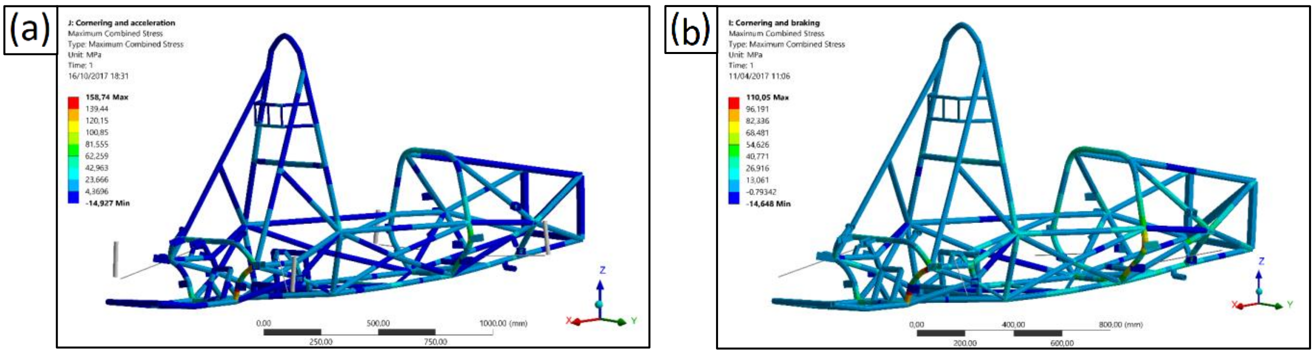

Figure 12. Maximum Combined Stress; (a) Cornering and acceleration, (b) Cornering and Braking.

For the analysis of torsional stiffness, we extracted the maximum point of deformation of the structure applying the condition explained in the procedure. The value and location of it can be seen in Fig. (13). The resulting stiffness was *2159.1 Nm / °*.

.

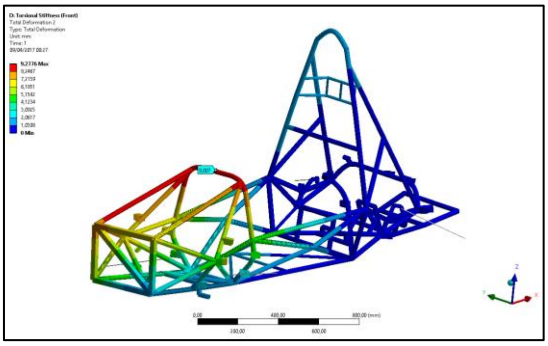

Figure 13. Maximum deformation in torsion.

The values obtained in the modal numerical analysis are represented in Tab. (3) in the section experimental results so that they can be compared with the values obtained experimentally with the purpose of validating the numerical model.

3.2 Experimental Results

In the torsional stiffness test, we extracted the applied force and torsion angle values by calculating the stiffness values. Moreover, we draw the Torsional Stiffness Diagram (1) by applied load.

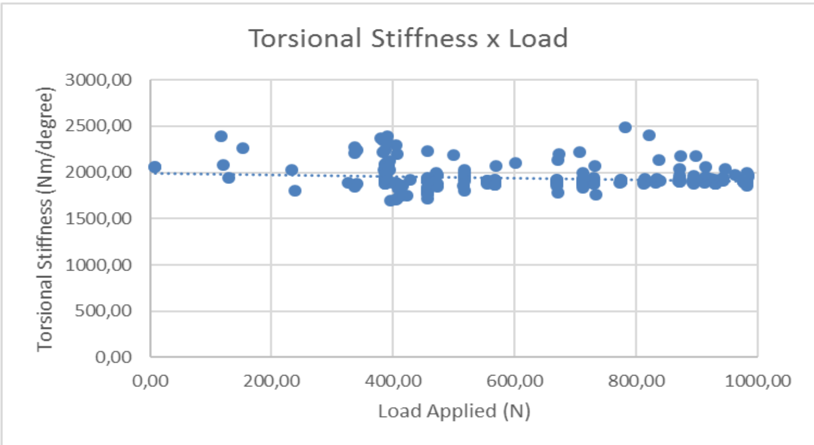

Diagram 1. Torsional Stiffess x Load.

As can be seen in Table 3, the values obtained in the numerical analysis and the modal test are compared. In addition, we calculated the percentage difference between the numerical and experimental values

Table 3. Numerical and experimental modal frequencies.

Modes	**Simulated Frequency (Hz)**	**Validated Frequency (Hz)**	**%**
Mode 7	38.049	41.367	8,72
Mode 8	57.393	57.795	0,70
Mode 9	66.425	68.119	2,55
Mode 10	73.869	74.549	0,92
Mode 11	82.330	82.989	0,80
Mode 12	90.424	92.413	2,20
Mode 13	92.705	94.503	1,94
Mode 14	120.760	122.076	1,09
Mode 15	128.040	130.652	2,04
		Average	2,33

4. CONCLUSIONS

Based on the data that we acquired on the structural analysis, we came up with the Tab. (4) to help us decide which material to use and how thick each tube needed to be.

Table 4. Material Selection.

Material	**1020**	**1045**	**4130**
Safety Factor	1.5	1.8	2.0
Cost/m*	1	2	19
Weldability	High	Medium	Low
Availability	High	Medium	Low

The SAE 1045 steel is easily tempered, which is risky to be use because of the fact that the structure is manufactured by the students on their own shop. And the SAE 4130 steel is 19 times more expensive than the SAE 1020. So the material chosen was SAE 1020 steel because of its weldability, for being available in regular markets and its achievable safety factor of 1.5 using the minimum thickness allowed on the rule T3.4 in most of the tubes.

As torsional loading and deformation of the chassis and suspension parts affect the drivability and performance of the car. To ensure performance and balance mass and rigidity. It was necessary to define how rigid the structure should be. And for this we rely on the SAE paper (Deakin, *et al.*, 2004). That says that for a car with a rolling rigidity of $1500Nm/°$, the lateral transfer of load begins to behave linearly in relation to the rolling rigidity for torsional stiffness of the chassis higher than *2000Nm / °*. Making suspension set-ups simpler and more efficient. Thus, the target of torsional stiffness was defined. From several numerical analyzes we look for this target and reaching this value we began the manufacturing process and validation of the structure with the torsional stiffness test presented in this work.

Comparing the values obtained in the modal analysis and assay we obtained a percentage difference below 3%, and with that the numerical model was validated.

5. ACKNOWLEDGEMENTS

We dedicate this work to all members of the SAE team of the São Carlos engineering school and to all the teachers and staff who have always been on hand to assist us.

6. REFERENCES

D. Seward, Race car design. London: Palgrave, 2014.
Deakin, A., Crolla, D., Ramirez, JP, and Hanley, R. 2004. The Effect of Chassis Stiffening on Race Car Handling Balance, Racing Chassis and Suspension Design, Society of Automotive Engineers, Warrendale, PA
SAE, Formula SAE Rules, SAE International, 2017-18.
William B. Riley and Albert R. George, 2001. Design, Analysis and Testing of a Formula SAE Car Chassis

7. RESPONSIBILITY NOTICE

The authors are the only responsible for the printed material included in this paper.